half-widths—decrease. Stark-broadening calculations have thus made possible a different and very convenient approach for determining the electron densities in dense plasmas from linewidth measurements with an accuracy comparable to other spectroscopic methods. The advantages of this method are that the temperature needs to be only roughly determined since the broadening is mainly a density effect, and that the width (and shift) measurements are quickly and rather precisely done, since only relative intensity measurements are required.

It is advisable to determine the widths of several lines to obtain a smaller statistical error. For example, the ratio of measured to calculated widths averaged over all six multiplets is in this experiment 1.00 with a standard deviation of ±0.06.

In comparing the cesium and oxygen experiments no significant deterioration in the results is observed, which means that the use of the Coulomb approximation does not seem to introduce additional significant errors in the case of a more complex atom.

Elastic and Inelastic Collision Cross Sections in Hydrogen and Deuterium from Transport Coefficients*

A. G. ENGELHARDT AND A. V. PHELPS

Westinghouse Research Laboratories, Pittsburgh, Pennsylvania

(Received 18 April 1963)

By means of a numerical solution of the Boltzmann equation, elastic and inelastic collision cross sections have been derived for electrons in H_2 and D_2 subjected to a dc electric field. The cross sections for momentum transfer, rotational excitation, vibrational excitation, electronic excitation, and ionization are investigated by comparing experimental and theoretical values of transport coefficients. The same momentum transfer cross section previously obtained for H_2 by Frost and Phelps has been found to be valid for D_2. Good agreement is secured between experiment and theory by multiplying the theoretical rotational cross sections of Gerjuoy and Stein by approximately 1.5, provided the polarization factor of Dalgarno and Moffett is used. The final cross section for vibrational excitation of H_2 has a threshold at 0.52 eV and a peak of 7.7×10^{-17} cm² at 4.5 eV, whereas that of D_2 has a threshold at 0.36 eV and a peak of 6.6×10^{-17} cm² at 4.7 eV. The derived electronic excitation cross sections are the same for both H_2 and D_2. The ionization cross section was taken from the experimental results of Tate and Smith. Calculated transport coefficients for electrons subjected to crossed electric and magnetic fields, and high-frequency ac electric fields are in agreement with recent experimental and theoretical results.

I. INTRODUCTION

ELASTIC and inelastic collisions of low-energy electrons with molecular gases have been the subject of considerable theoretical and experimental investigation[1–3] in recent years. In this paper we extend the cross-section determinations of Frost and Phelps[4] to higher energies in H_2, and to D_2. We include the processes of elastic scattering, and rotational, vibrational, and electronic excitation as well as ionization. Stated somewhat differently, we shall take into account both elastic and inelastic collisions involving electrons with energies up to 100 eV.

Our method of calculation is essentially the same as that of Frost and Phelps (hereafter called I). We numerically solve the Boltzmann transport equation for the distribution function, f, of electron energies taking into consideration both elastic and inelastic collisions. In the case of only a dc electric field present the three transport coefficients[5] of principal interest are the diffusion-coefficient, D, the mobility, μ, and the Townsend primary ionization coefficient α_i. These coefficients are found by taking the appropriate average over f. Cross sections are determined by successive adjustments to initial estimates until theoretical and experimental values of the transport coefficients are brought into good agreement. The results are by no means unique, but they certainly do represent a consistent and realistic set of elastic and inelastic collision cross sections.

It is possible to consider separately three distinct regions of electron energy. In our calculation the electron energy is characterized by an experimentally measurable quantity, the characteristic energy ϵ_K, where

$$\epsilon_K = eD/\mu, \tag{1}$$

and e is the electronic charge.

[1] D. R. Bates, *Atomic and Molecular Processes* (Academic Press Inc., New York, 1962).
[2] H. S. W. Massey and E. H. S. Burhop, *Electronic and Ionic Impact Phenomena* (Clarendon Press, Oxford, England, 1952).
[3] L. B. Loeb, *Basic Processes in Gaseous Electronics* (University of California Press, Berkeley, California, 1955).
[4] L. S. Frost and A. V. Phelps, Phys. Rev. **127**, 1621 (1962).
[5] W. P. Allis, in *Handbuch der Physik*, edited by S. Flügge (Springer-Verlag, Berlin, 1956), Vol. 21, p. 383.

In the first region (A), ϵ_K ranges from its thermal value to that where vibrational excitation first must be taken into consideration. In this region we assume for H_2 the same cross section Q_m for momentum transfer collisions as previously found in I. The thresholds and shapes of the cross sections for rotational excitation are based on the theories of Gerjuoy and Stein (GS)[6] as modified by Dalgarno and Moffett (DM).[7] In particular, we have investigated the question of whether including the polarization correction improves the agreement between theory and experiment. It is to be expected that this correction, which arises from the polarization of the H_2 molecule and increases the rotational cross section, would reduce the discrepancy between theory and experiment discussed in I. There it was concluded that although the shapes and thresholds of the GS rotational cross sections appeared to be correct, the amplitude had to be multiplied by a factor of 1.7. Furthermore, we have performed calculations for electrons in D_2 in this energy range using the same cross sections for elastic scattering and the same theory for rotational excitation, as for H_2. In the case of rotational excitation, appropriate allowance is made for the different atomic mass and statistical weights of H_2 and D_2.

In the second region (B), ϵ_K varies from the energy where vibrational excitation first assumes importance to that where dissociation first begins to become of significance. Using previously derived cross sections for elastic scattering[4] and rotational excitation we are able to derive for both H_2 and D_2 the rising part of the cross section for vibrational excitation. Specifically this cross section is determined by a comparison of calculated and experimental transport coefficients involving μ and D.

In the third and highest energy régime (C), elastic scattering and vibration, electronic excitation, and ionization are considered. For both H_2 and D_2 the high-energy portion of the momentum transfer and ionization cross sections are taken from the results of Brode,[8] and Tate and Smith,[9] respectively. By a comparison of calculated and experimental values of α_i, we have been able to determine the cross sections for electronic excitation and to some extent the falling part of the vibrational cross section. This analysis is based on the postulate that the electronic excitation cross sections are the same for both H_2 and D_2. The analysis in this energy range is similar in many respects to those of Lunt and Meek,[10] Corrigan and von Engel,[11] and Heylen and Lewis.[12] Our approach differs from that used by

these authors in that we choose to ignore the experimental values of ϵ_K for $\epsilon_K > 1$ eV and base our analysis on the other measured transport coefficients. As a result we obtain reasonable cross sections for elastic and inelastic scattering using electron distribution functions which are more realistic than the Maxwellian distribution.

As a final check on our results we have computed transport coefficients for electrons in H_2 and D_2 subjected to crossed electric and magnetic fields, and ac electric fields. A comparison of these coefficients with recent experimental[13] and theoretical[14] findings lends additional support to the accuracy of our derived cross sections.

II. BOLTZMANN EQUATION AND TRANSPORT INTEGRALS

In this section we present the equations pertinent to this analysis and discuss our method of solution. Since our technique differs very little from that used in I, we shall refrain from any derivations, but shall emphasize the salient points.

The basis of our treatment is the Boltzmann equation for the distribution function of electrons in a parent neutral gas. We write it in the form

$$\frac{d}{d\epsilon}\left(\frac{e^2 E_\epsilon^2 \epsilon}{3NQ_m}\frac{df}{d\epsilon}\right) + \frac{2m}{M}\frac{d}{d\epsilon}\left(\epsilon^2 NQ_m\left[f + kT\frac{df}{d\epsilon}\right]\right)$$

$$+ \sum_i \left[(\epsilon + \epsilon_j)f(\epsilon + \epsilon_j)NQ_j(\epsilon + \epsilon_j) - \epsilon f(\epsilon)NQ_j(\epsilon)\right]$$

$$+ \sum_i \left[(\epsilon - \epsilon_j)f(\epsilon - \epsilon_j)NQ_{-j}(\epsilon - \epsilon_j)\right.$$

$$\left. - \epsilon f(\epsilon)NQ_{-j}(\epsilon)\right] = 0. \quad (2)$$

In this equation, ϵ is the electron energy[15] $= \frac{1}{2}mv^2$, (where v is the electron speed), N the neutral molecule density, Q_m the cross section for momentum transfer collisions, m and M are the electron and molecule masses, respectively, and f is normalized by

$$\int_0^\infty \epsilon^{1/2} f(\epsilon) d\epsilon = 1. \quad (3)$$

The energy-dependent effective electric field E_ϵ has been shown by Allis[5] to be given by the relation

$$E_\epsilon^2 = Q_m^2(\epsilon)E^2[Q_m^2(\epsilon) + (\Omega/N)^2 m/2e]^{-1}, \quad (4)$$

where E is the dc electric field. In the case of mutually

[6] E. Gerjuoy and S. Stein, Phys. Rev. **97**, 1671 (1955); **98**, 1848 (1955).

[7] A. Dalgarno and R. J. Moffett, Indian Academy of Sciences Symposium on Collision Processes, 1962 (unpublished).

[8] R. B. Brode, Rev. Mod. Phys. **5**, 257 (1933).

[9] J. T. Tate and P. T. Smith, Phys. Rev. **39**, 270 (1932).

[10] R. W. Lunt and C. A. Meek, Proc. Roy. Soc. (London) **A157** 146 (1936).

[11] S. J. B. Corrigan and A. von Engel, Proc. Roy. Soc. (London) **A245**, 335 (1958).

[12] A. E. D. Heylen and T. J. Lewis, in *Proceedings of the Fourth International Conference on Ioinzation Phenomena in Gases* (North-

Holland Publishing Company, Amsterdam, 1960), Vol. I, p. 156. See also, A. E. D. Heylen, Proc. Phys. Soc. (London) **76**, 779 (1960).

[13] M. J. Bernstein, Phys. Rev. **127**, 335 and 342 (1962); and W. B. Cottingham and S. J. Buchsbaum, Phys. Rev. **130**, 1002 (1963). See also Ref. 47.

[14] G. A. Pearson and W. B. Kunkel, Lawrence Radiation Laboratory Report UCRL-10366, 1962 (unpublished). See also Phys. Rev. **130**, 864 (1963).

[15] Rationalized mks units are used throughout. Any exceptions are specifically denoted.

perpendicular or "crossed" dc electric and magnetic fields

$$\Omega = \omega_b = eB/m, \qquad (5)$$

where B is the magnetic field and ω_b is the electron cyclotron frequency. For the situation of a high-frequency ac electric field of radian frequency ω, $\Omega = \omega$. In addition, in Eq. (2) Q_j is the cross section for electron energy loss in excitation of the jth level, Q_{-j} the cross section for electron energy gain in the de-excitation of the jth level, and ϵ_j is the energy loss associated with the jth level.

This particular form of the Boltzmann equation is an extension discussed in I of the earlier results of Holstein[16] and Margenau[17] to include inelastic collisions of the second kind, i.e., the last term in Eq. (2). It is worth noting from Eq. (4) that in the limit of extremely small magnetic fields $E_\epsilon \propto E$, whereas in the limit of extremely large magnetic fields, $E_\epsilon \propto E/B$.

We can associate with each term in the Boltzmann equation the gain or loss of energy due to one of the processes being considered. The first term represents the effect of energy input to the electrons from the field, the second term energy loss and gain (in that order) in elastic collisions, the third term energy loss in inelastic collisions of the first kind, and the fourth term represents energy gain in inelastic collisions of the second kind.[18] Near thermal equilibrium when the mean electron energy is close to that of the gas and the distribution function is Maxwellian, the energy lost in elastic collisions is balanced by the energy gained in elastic collisions. A similar situation must occur also for inelastic collisions, viz., Q_j and Q_{-j} are related by detailed balancing.[18]

Two techniques are employed for solving the Boltzmann equation corresponding to two regions of ϵ_K. In region A as defined in Sec. I, ϵ_K is of the order of its thermal equilibrium value, kT, and inelastic energy gained by the electrons cannot be neglected, i.e., collisions of the second kind are important. In this case at a given energy the distribution function has contributions from electrons which have lost and gained energy by inelastic processes. Therefore, in order to solve the Boltzmann equation we write it in finite difference form obtaining a set of linear algebraic equations for f, which is then solved by standard techniques.[4]

In regions B and C, ϵ_K is large enough so that the results are independent of the gas temperature. Under these conditions a temperature is chosen such that collisions of the second kind are neglected. The Boltzmann equation can then be solved by backward prolongation[4,19]; viz., by assuming that for sufficiently high energy, f is given primarily by the elastic terms, one

then proceeds to prolong this high-energy solution backwards in energy taking into account both elastic and inelastic collisions.

The determination of cross sections arises from a comparison of experimental and theoretical values of various combinations of transport coefficients all of which we normalize to the neutral particle density. The diffusion coefficient D is given by

$$DN = (2/m)^{1/2}/3 \int_0^\infty f(\epsilon)\epsilon d\epsilon/Q_m(\epsilon). \qquad (6)$$

The two mobilities of interest μ_1 and μ_2 are obtained from the expressions

$$\mu_1 N = -\frac{e(2/m)^{1/2}}{3}$$

$$\times \int_0^\infty \frac{\epsilon Q_m(\epsilon)}{Q_m^2(\epsilon) + (\Omega/N)^2(m/2\epsilon)} \frac{df}{d\epsilon}d\epsilon = \frac{w_1}{E/N}, \qquad (7)$$

and

$$\mu_2 N = -\frac{e}{3}\frac{\Omega}{N}\int_0^\infty \frac{\epsilon^{1/2}}{Q_m^2(\epsilon) + (\Omega/N)^2(m/2\epsilon)}\frac{df}{d\epsilon}d\epsilon = \frac{w_2}{E/N}. \qquad (8)$$

If $\Omega = \omega_b$, $\mu_1 = \mu_T$ and $w_1 = w_T$, the mobility and drift velocity, respectively, transverse to the magnetic field, but parallel to the electric field. Also, in this case, $\mu_2 = \mu_\perp$ and $w_2 = w_\perp$, the mobility and drift velocity, respectively, perpendicular to both electric and magnetic fields; D is then the diffusion coefficient parallel to the magnetic field. From Eq. (8) it can be shown that in the limit of high-magnetic fields $w_\perp \rightarrow E/B$. If $\omega_b = 0$, we can write $\mu_\perp = w_\perp = 0$, and $\mu_T = \mu = w/E$, where μ and w are the mobility and drift velocity in the absence of a magnetic field.

If Eq. (2) is multiplied by $(2/m)^{1/2}\epsilon d\epsilon$ and integrated over all energies the energy balance equation is obtained in the form,[4]

$$eEw_1 = \left(\frac{2}{m}\right)^{1/2}\frac{2m}{M}\int_0^\infty \epsilon^2 NQ_m(\epsilon)\left[f(\epsilon) + kT\frac{df(\epsilon)}{d\epsilon}\right]d\epsilon$$

$$+\left(\frac{2}{m}\right)^{1/2}\sum_j \epsilon_j \int_0^\infty \epsilon f(\epsilon)[NQ_j(\epsilon) - NQ_{-j}(\epsilon)]d\epsilon. \qquad (9)$$

This equation states that the power input to the electrons from the field, eEw_1, is balanced by the power dissipated by the electrons in elastic and inelastic collisions, viz., the first and second integrals, respectively, on the right-hand side. Consequently, once the Boltzmann equation has been solved we can determine the power input to each of the elastic and inelastic processes and obtain simultaneously a check on the self-consistency of the computation. Such a check was made

[16] T. Holstein, Phys. Rev. 70, 367 (1946).
[17] H. Margenau, Phys. Rev. 69, 508 (1946).
[18] A. C. G. Mitchell and M. W. Zemansky, Resonance Radiation and Excited Atoms (Cambridge University Press, New York, 1934).
[19] B. Sherman, J. Math. Analysis Application 1, 342 (1960).

for each solution of Eq. (2) for f and solutions were considered acceptable only when the two sides of Eq. (9) were equal to within one part in 10^4 of eEw_1.

We define a frequency coefficient for the lth inelastic process from Eq. (9) as,

$$\nu_l/N = (2/m)^{1/2} \int_0^\infty \epsilon f(\epsilon) Q_l(\epsilon) d\epsilon. \qquad (10)$$

Thus, for example, in the case of ionization the ionization frequency ν_i is determined by an evaluation of the power input by the electrons to the ionization process. For only a dc electric field present, the comparison between theory and experiment is made in terms of a coefficient α_l for the lth inelastic process given by

$$\alpha_l/N = (1/w)\nu_l/N. \qquad (10a)$$

In regions A and B our procedure in evaluating elastic and inelastic collision cross sections is to define an effective elastic collision frequency ν_m and an energy exchange collision frequency ν_u by the relations,

$$\nu_m/N = (e/m)(1/\mu N) = (e/m)[(E/N)/w], \qquad (11)$$

and

$$\nu_u/N = [ew(E/N)]/(\epsilon_K - kT). \qquad (12)$$

The quantity ν_m is sensitive primarily to changes in the elastic cross section,[4] and is affected only mildly by changes in the inelastic cross sections used. From Eq. (12) ν_u is defined as the power input per electron due to the electric field divided by the excess of electron energy over its thermal equilibrium value, i.e., $\epsilon_K - kT$, and is most sensitive to changes in the inelastic collision cross sections.[4] In this manner we are able to separate to a large degree the effects of elastic and inelastic collisions. Our procedure then is to plot experimental and theoretical values of ν_m and ν_u versus ϵ_K, and to make the appropriate adjustments in the elastic and inelastic cross sections until a satisfactory fit is obtained.

On the other hand, for lack of adequate experimental data in region C, the highest energy region, we have derived cross sections applicable to this region on the basis of agreement between experimental and calculated values of α_i only. As a result, we obtain inelastic collision cross sections in this region which are somewhat dependent on the assumed momentum transfer cross section.

III. DETERMINATION OF CROSS SECTIONS

As stated in the Introduction, our procedure for determining cross sections can be subdivided into three separate techniques corresponding to three regions of ϵ_K, viz., regions A, B, and C as discussed in the Introduction. This subdivision is facilitated by the fact that the cross sections derived for a given region are reasonably independent of those for the neighboring region.

Region A. Rotational Excitation and Elastic Scattering $[(kT/e) < \epsilon_K < 0.08 \text{ eV}]$

The cross sections we use for rotational excitation are derived from the theory of Gerjuoy and Stein[6] who considered the problem of the rotational excitation of a homonuclear molecule by low energy electrons; the interaction mechanism was taken to be the long range quadrupole interaction. For both H_2 and D_2 the cross section $Q_{J,J+2}(\epsilon)$ for electron energy loss in rotationally exciting a molecule from the Jth to the $(J+2)$nd level is

$$Q_{J,J+2} = (p_J/P_r)\sigma_{J,J+2} \exp(-E_J/kT). \qquad (13)$$

The factor[20] $(p_J/P_r) \exp(-E_J/kT)$ represents the fraction of the molecules in the Jth rotational level where

$$p_J = (2t+1)(t+a)(2J+1), \qquad (14)$$

t is the nuclear spin[20] ($\frac{1}{2}$ for H_2 and 1 for D_2), and

$$\begin{aligned} a &= 0, \quad J \text{ even}, \\ &= 1, \quad J \text{ odd}. \end{aligned} \qquad (15)$$

In Eq. (13), E_J is the Jth energy level of the rotating molecule given by

$$E_J = J(J+1)B_0, \qquad (16)$$

where B_0 is the rotational constant[21] (0.00754 eV for H_2 and 0.00377 eV for D_2),

$$P_r = \sum_J p_J \exp(-E_J/kT), \qquad (17)$$

$$\sigma_{J,J+2}(\epsilon) = \frac{(J+2)(J+1)}{(2J+3)(2J+1)}\sigma_0\left[1 - \frac{(4J+6)B_0}{\epsilon}\right]^{1/2}, \qquad (18)$$

and

$$\sigma_{J,J-2}(\epsilon) = \frac{J(J-1)}{(2J-1)(2J+1)}\sigma_0\left[1 + \frac{(4J-2)B_0}{\epsilon}\right]^{1/2}, \qquad (19)$$

where

$$\sigma_0 = 8\pi \mathcal{Q}^2 a_0^2/15, \qquad (20)$$

$\mathcal{Q}$ is the electric quadrupole moment in units of ea_0^2, and a_0 is the Bohr radius. Equation (18) gives the cross section for an electron energy loss[22] of

$$\epsilon_J = (4J+6)B_0. \qquad (21)$$

This cross section increases rapidly near the threshold energy ϵ_J, and for large energies asymptotically approaches a constant value as shown in Fig. 1 for H_2. On the other hand, Eq. (19) gives the cross section for an electron energy gain of

$$\epsilon_{-J} = (4J-2)B_0. \qquad (22)$$

These rotational cross sections are substantially greater

[20] A. Farkas, *Orthohydrogen, Parahydrogen, and Heavy Hydrogen* (Cambridge University Press, New York, 1935).
[21] G. Herzberg, *Spectra of Diatomic Molecules* (D. Van Nostrand Company, Inc., Princeton, New Jersey, 1950), pp. 532 and 553.
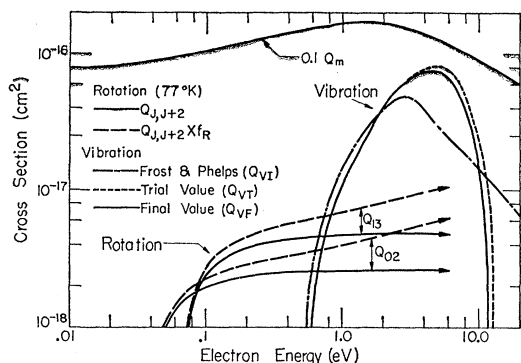[22] The selection rule is $\Delta J = \pm 2$.

FIG. 1. Momentum transfer, rotational excitation, and vibrational excitation cross sections for electrons in H_2 as a function of electron energy. Q_m is the momentum transfer cross section and is the same as that previously derived by Frost and Phelps. The rotational cross sections are for 77°K and inelastic collisions of the first kind; the solid lines indicate the rotational cross sections calculated based on the theory of Gerjuoy and Stein, and the dashed lines show the effect of multiplying by the polarization factor f_R of Dalgarno and Moffet. The final value of the vibrational cross section Q_{VF} is shown by the solid line, whereas the short dash-long dash curve shows the vibrational cross section Q_{VI} reported previously by Frost and Phelps. The dashed vibrational cross section Q_{VT} is used to illustrate the effect on the ionization coefficient of varying the vibrational cross section.

than those previously estimated by Morse[23] and Carson.[23]

Dalgarno and Moffett[7] give $0.473ea_0^2$ as the effective value of the quadrupole moment for H_2 to be used in Eq. (20). This value is based on the measurements of Harrick and Ramsey[24] with allowance for nuclear motion. Although Frost and Phelps[4] were able to substantiate both the shape and threshold values of the GS rotational cross section, they had to use an effective quadrupole moment of $0.62ea_0^2$. This discrepancy could not be explained. Furthermore, DM find that the GS rotational cross sections should be multiplied by a factor $f_R(\epsilon)$ due to the polarization of the molecule. This factor which is greater than unity for H_2 and D_2 is given by the expression

$$f_R(\epsilon) = 1 + \frac{P_\alpha(4\epsilon - \epsilon_J)}{\epsilon^{1/2}} + \frac{9}{4}P_\alpha^2(2\epsilon - \epsilon_J), \quad (23)$$

where

$$P_\alpha = \frac{\pi(\alpha_{11} - \alpha_\perp)}{24\mathcal{Q}R^{1/2}}. \quad (24)$$

In Eq. (24), α_{11} and $\alpha_\perp$ are the parallel and perpendicular polarization constants in units of a_0^3, and R is the Rydberg constant. It is the purpose of this section to determine to what extent the polarization correction obviates the discrepancy found in I. In addition, we are able to verify the momentum transfer cross section applicable to region A.

Shown in Figs. 1 and 2 for both H_2 and D_2 are the cross sections for elastic scattering and for rotational

[23] P. M. Morse, Phys. Rev. 90, 15 (1953); and T. R. Carson, Proc. Phys. Soc. (London) A67, 908 (1954).
[24] N. J. Harrick and N. F. Ramsey, Phys. Rev. 88, 228 (1952).

excitation. We have used the same Q_m for H_2 and D_2. In the case of rotational excitation at 77°K, we show only two cross sections for inelastic collisions of the first kind, viz., Q_{02} and Q_{13}. The values of $Q_{J,J+2}$ for excitation to higher states and those of $Q_{J,J-2}$ for collisions of the second kind are considerably smaller in magnitude and are not shown. For example, for H_2, $[Q_{20}/Q_{02}]_{\epsilon=\infty} \cong 10^{-3}$; on the other hand, since the rotational constant for D_2 is half as large as that for H_2, $[Q_{20}/Q_{02}]_{\epsilon=\infty} \cong 0.03$. Thus, inelastic collisions of the second kind are more important for D_2 than for H_2. Nevertheless, in our calculation for this region we have taken collisions of the second kind into account for both gases. Had the calculations been performed for a higher gas temperature, higher states would have had to be considered.

The effect of the polarization correction can be seen from Fig. 1 where for comparison we have plotted the rotational cross sections for H_2 both with and without f_R. We have used the same magnitude factor[25] M_R to multiply $Q_{J,J+2}$ in all four cases, and a quadrupole moment of 0.473 in f_R. The polarization correction increases the effective rotational cross section by about 10% near threshold and 30% near the onset of vibrational excitation at 0.52 eV. Figure 2 displays the differences in the rotational cross sections of H_2 and D_2.

As in I the influence of changes in elastic and inelastic cross sections is evaluated from plots of ν_u/N and ν_m/N versus ϵ_K in eV as shown in Figs. 3 and 4. For the moment we are concerned only with the region of rotational and elastic scattering, i.e., $\epsilon_K < 0.08$ eV. Figure 3 exhibits plots of ν_m/N and ν_u/N for H_2 both with and without the polarization correction, and for several values of M_R; similar plots for D_2 are shown in Fig. 4. Our calculations are shown as points, whereas the smooth curves represent an average of the best available experimental data.[4]
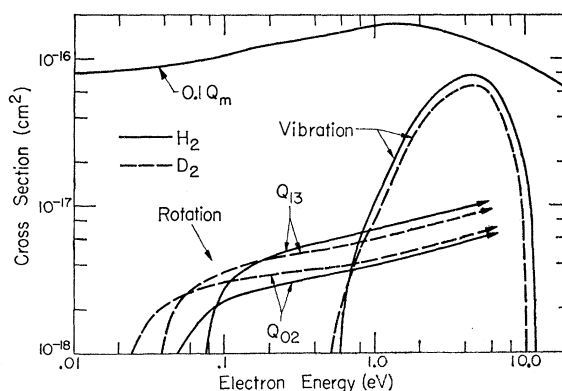

FIG. 2. Momentum transfer, rotational excitation, and vibrational excitation cross sections for electrons in H_2 and D_2 as a function of electron energy. The same momentum transfer cross section is used for both H_2 and D_2. Shown are the cross sections for rotational excitation at 77°K which include the polarization factor of Dalgarno and Moffett.

[25] We define M_R as the energy-independent factor by which $Q_{J,J+2}$ is multiplied, e.g., in I, $M_R = 1.73$ for $\mathcal{Q} = 0.473ea_0^2$.
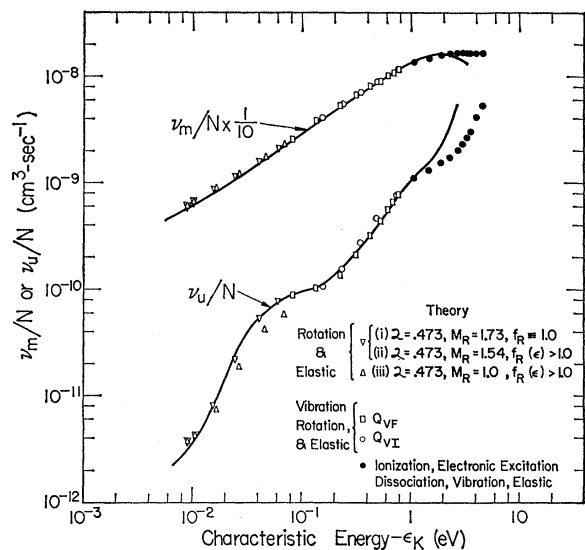
FIG. 3. Elastic collision ν_m/N and energy exchange ν_u/N frequencies for H_2 at 77°K plotted against the characteristic energy ϵ_K. The points represent our theoretical calculations and the smooth curves represent an average of the best available experimental data. In the region where $\epsilon_K < 0.08$ eV we show results for three combinations of the quadrupole moment $\mathcal{Q}$, the magnitude factor M_R, and the polarization factor f_R. The first two cases yield identical values. In the region where vibration, rotation, and elastic scattering are considered, we have plotted results obtained using our final vibrational cross section Q_{VF} and the one Q_{VI} previously reported by Frost and Phelps. For $\epsilon_K > 1.0$ eV we take into consideration ionization, photon excitation, dissociation, vibration, and elastic scattering but neglect rotation.

In order to demonstrate the effects of f_R, we show in Fig. 3 the results of calculations for three distinct cases:

(i) $\mathcal{Q}=0.473$, $M_R=1.73$, $f_R\equiv1.0$,

(ii) $\mathcal{Q}=0.473$, $M_R=1.54$, $f_R(\epsilon)>1.0$,

(iii) $\mathcal{Q}=0.473$, $M_R=1.0$, $f_R(\epsilon)>1.0$.

For all three cases the values of ν_m/N lie close to the experimental curve; this result is consistent with the findings of I where it was concluded that in H_2 relatively small changes in the inelastic collision cross sections did not alter the agreement between experimental and theoretical values of ν_m/N. This conclusion is also true for the calculations of regions B and C. In the case of the ν_u/N curve we obtain good agreement between theory and experiment for cases (i) and (ii); in fact, the results for these two cases are virtually the same since the increase in case (i) of the rotational cross section caused by setting $M_R=1.73$ is offset by taking $f_R\equiv1.0$. On the other hand, it clearly does not suffice to use the polarization correction with $M_R=1.0$ since the points of case (ii) are well below the experimental curve. We note that all three cases yield the same result in the near thermal region where rotational excitation is of less significance. We conclude, therefore, that the inclusion of the polarization factor reduces the error in the effective quadrupole moment to about 25% but that the remaining discrepancy is outside the experimental error.

In the case of D_2 we also choose three illustrative cases as follows:

(i) $\mathcal{Q}=0.473$, $M_R=1.73$, $f_R\equiv1.0$,

(ii) $\mathcal{Q}=0.473$, $M_R=1.73$, $f_R(\epsilon)>1.0$,

(iii) $\mathcal{Q}=0.473$, $M_R=1.47$, $f_R(\epsilon)>1.0$.

Here we have used the same value for the effective quadrupole moment as for H_2. Presumably the correction to the value measured by Barnes, Bray, and Ramsey[26] for nuclear motion will be somewhat lower than for H_2. Unfortunately, this correction has not been calculated. [Note added in proof. R. J. W. Henry and A. Dalgarno (private communication) have found that the corrected quadrupole moment for D_2 is the same as for H_2.] We do not show the ν_m/N points for case (ii) since they almost coincide with those for the other two cases shown. In any event, acceptable agreement is achieved in all three cases between calculated and experimental values of ν_m/N; hence, we conclude that our assumption of the same elastic cross section for both H_2 and D_2 in this region is justified to a large extent. Of possibly greater interest is the ν_u/N plot from which it can be seen that cases (i) and (iii) give much the same result for $\epsilon_K < 0.02$ eV; however, above 0.02 eV to the onset of vibrational excitation the results for case (i) seem to suffer a rather disconcerting droop. A comparison of cases (ii) and (iii) reveals that, although case (ii) furnishes a slightly better fit in the near thermal region ($\epsilon_K < 0.015$ eV), above 0.015 eV the agreement is un-
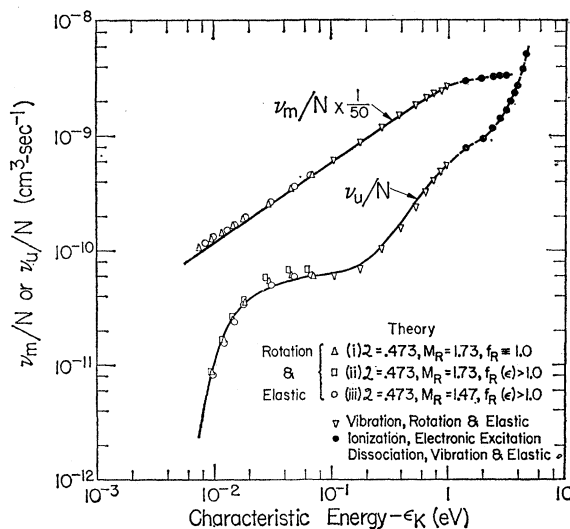

FIG. 4. Elastic collision and energy exchange frequencies for D_2 at 77°K plotted against ϵ_K in eV. As in Fig. 3 the points represent our theoretical calculations and the smooth curves are an average of the best available experimental data. Above $\epsilon_K=1.0$ eV the dashed curves represent calculated results since no experimental data are available for this region.

[26] R. G. Barnes, P. J. Bray and N. F. Ramsey, Phys. Rev. 94, 893 (1954). The quadrupole moment given by these authors for D_2 is the same as for H_2 to within experimental error.

satisfactory compared to that of case (iii) which, consequently, we consider to be the best solution.

Our final comparison for this region is in terms of graphs of w and ϵ_K versus E/N as shown in Fig. 5 for H_2 and Fig. 6 for D_2. We show our calculations as smooth curves, i.e., cases (i) and (ii) for H_2 and case (iii) for D_2; the various experimental results[27-34] appear as points. The agreement is excellent for H_2, since the discrepancy for both w and ϵ_K is less than 5%. In the case of D_2, the use of the same theory for rotational excitation and the same momentum transfer cross section as for H_2 leads to agreement for w and ϵ_K to within 10%. This residual discrepancy appears to arise from an error of as much as 20% in the shape of the theoretical rotational cross section.

Region B. Vibration, Rotation, and Elastic Scattering ($0.08 < \epsilon_K < 1.0$ eV)

When ϵ_K exceeds a value of approximately 0.08 eV, there are a sufficient number of electrons in the distribution function whose energies exceed the threshold for vibrational excitation to necessitate considering vibrational excitation in the solution of Eq. (2) for the distribution function. For H_2 and D_2 this threshold[21] occurs at 0.516 and 0.360 eV, respectively. Because in this region $\epsilon_K \gg kT$, we neglect the effect of inelastic collisions
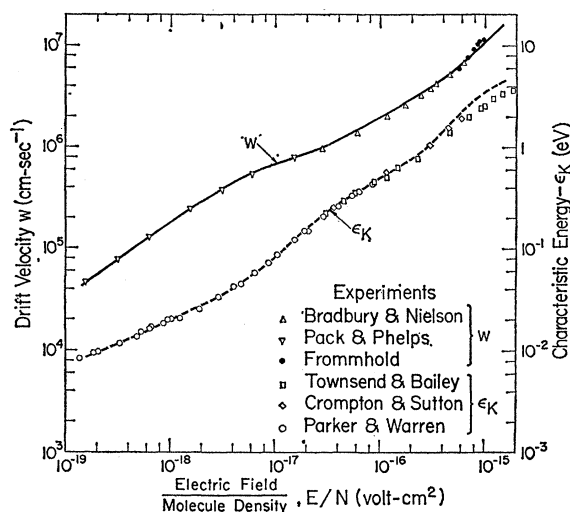

FIG. 5. Drift velocity, w and characteristic energy ϵ_K for H_2 at 77°K as a function of E/N. The points represent experimental results and the smooth curves our computations. The calculated w and ϵ_K curves were obtained using $\mathcal{Q}=0.473$, $M_R=1.54$, and $f_R(\epsilon)>1.0$.

[27] N. E. Bradbury and R. A. Nielsen, Phys. Rev. 49, 388 (1936).
[28] J. L. Pack and A. V. Phelps, Phys. Rev. 121, 798 (1961).
[29] L. Frommhold, Z. Physik 160, 554 (1960).
[30] J. S. Townsend and V. A. Bailey, Phil. Mag. 42, 873 (1921).
[31] R. W. Crompton and D. J. Sutton, Proc. Roy. Soc. (London) A215, 467 (1952).
[32] R. W. Warren and J. H. Parker, Phys. Rev. 128, 2661 (1962).
[33] J. L. Pack, R. E. Voshall, and A. V. Phelps, Phys. Rev. 127, 2084 (1962).
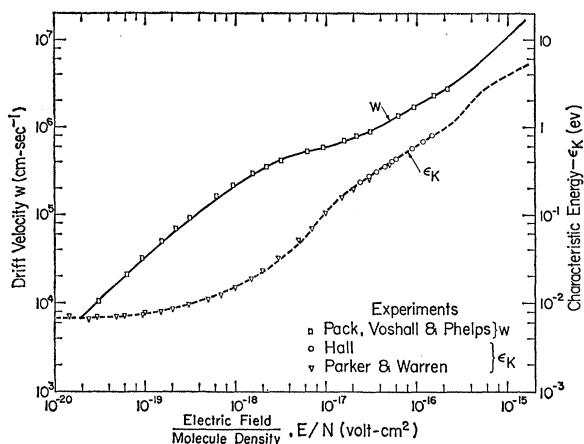[34] B. I. H. Hall, Australian J. Phys. 8, 468 (1955).

FIG. 6. Drift velocity and characteristic energy for D_2 at 77°K as a function of E/N. The points represent experimental results and the smooth curves our computations. The calculated w and ϵ_K curves were obtained using $\mathcal{Q}=0.473$, $M_R=1.47$, and $f_R(\epsilon)>1.0$.

of the second kind and, consequently, are able to solve the Boltzmann equation by the method of backward prolongation.[4,19]

Figures 1 and 2 show the cross sections Q_V used for vibrational excitation. For this region of ϵ_K we are able to determine with reasonable accuracy the rising part of the cross section for vibrational excitation up to approximately 4 eV for both H_2 at D_2. In all of our calculations we have assumed that only the first vibrational level is excited. If higher levels are excited, the sum of the vibrational-excitation cross sections will be smaller than our Q_V. Figure 1 shows two vibrational cross sections for H_2 which we have used in region B. The first, Q_{VI}, is that reported in I and was constructed so as to pass through the experimental results of Ramien[35]; the second, Q_{VF}, represents our final value and gives a better fit to experimental data. Below 3 eV, Q_{VF} is not substantially different from Q_{VI}; nevertheless, the effect of the difference is determined readily by our analysis. Figure 2 displays a comparison of the vibrational cross sections of H_2 and D_2. Below 0.7 eV, the D_2 cross section is greater than that of H_2. On the other hand, in order to obtain good agreement between experimental and theoretical values of ν_u/N, it has been necessary above 0.7 eV to assign H_2 a cross section approximately 20% greater than that of D_2.

In performing calculations for this range using our final vibrational cross sections for H_2 and D_2, we have employed values of $\mathcal{Q}, M_R$, and f_R corresponding to case (ii) of H_2 and case (iii) of D_2, i.e., those values which gave the best fit in region A. The calculations done using Q_{VI} assumed the same rotational cross section as in I,

[35] H. Ramien, Z. Physik 70, 353 (1931). See also K. T. Chao, S. F. Wang, and K. C. Shen, Sci. Record (Peking) 2, 358 (1949). These authors obtain values somewhat larger than Ramien. Theoretical calculations of the vibrational excitation cross section are one to two orders of magnitude smaller than the experimental values. See for example, T. Y. Wu, Phys. Rev. 71, 111 (1947); H. S. W. Massey, Trans. Faraday Soc. 31, 556 (1935); and Ref. 23.
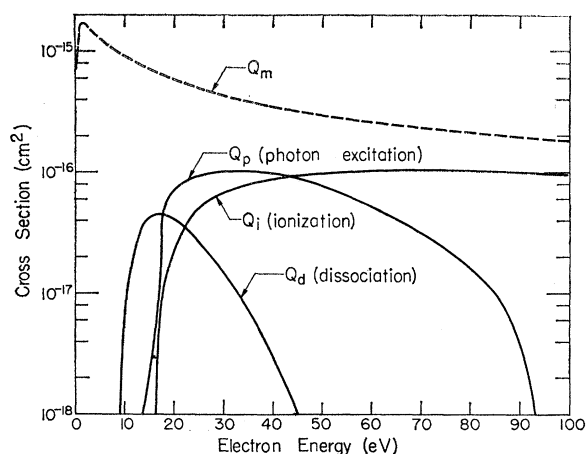
FIG. 7. Momentum transfer, dissociation, photon excitation, and ionization cross sections for electrons in both H_2 and D_2 as a function of electron energy.

i.e., case (i) of H_2. Our results in terms of the ν_m/N plots are shown on Fig. 3 for H_2 and Fig. 4 for D_2. The closeness of our calculated ν_m/N points to the experimental curves for the two H_2 and the one D_2 vibrational cross sections justifies the Q_m used. The effect of varying the vibrational cross section of H_2 can be deduced from the ν_u/N plot of Fig. 3. At the low-energy end of region B, viz., $0.08 < \epsilon_K < 0.2$ eV, the fit has been improved over that in I primarily because of the introduction of the polarization correction which causes the rotational cross section to increase with energy rather than approach an asymptotic limit. On the other hand, for $0.2 < \epsilon_K < 1.0$ eV, the ν_u/N points calculated using Q_{VI} fall approximately 10–15% above the curve, whereas Q_{VF} has been adjusted to give as good a fit as possible.[36] A similar procedure of adjusting the D_2 vibrational cross section to maximize agreement resulted in the satisfactory fit of the ν_u/N plot in Fig. 4. The final comparison made in terms of w and ϵ_K as shown in Fig. 5 for H_2 and Fig. 6 for D_2 indicates very little discrepancy.

Region C. Vibration, Dissociation, Electronic Excitation, Ionization, and Elastic Scattering ($\epsilon_K > 1.0$ eV)

Our method of analysis for region C, the highest energy régime considered, is substantially different from that used for regions A and B. In part, this different approach arises from the lack of sufficiently reliable experimental values of ϵ_K for H_2. Thus, an effort to determine the inelastic cross sections in this energy range by the procedure used at lower values of ϵ_K led to unreasonably large values for the cross sections and to ionization coefficients which were much to small. More-

over, in the case of D_2 there are no experimental results for these two transport coefficients. Fortunately, there have been reported a number of experimental determinations of α_i, the Townsend primary ionization coefficient. The principle drawback to using only α_i to determine cross sections is that no separation is achieved between elastic and inelastic effects. Consequently, the inelastic cross sections we have derived are dependent on the Q_m employed.

Shown in Figs. 2 and 7 are the curves representing our final values of the collision cross sections. The cross section for momentum transfer collisions has been taken from the results of Brode.[8] The ionization cross section is the same as that reported by Tate and Smith.[9] The only direct measurement of electronic-excitation cross sections for H_2 is that of Ramien[35] for energies between 8.85 and 12 eV. This cross section is presumably that for excitation of the $b^3\Sigma_u^+$ state which results in dissociation of the hydrogen molecule.[37] One expects the excitation of higher electronic states of H_2 to begin at about 11.5 eV and to include cross sections of both triplet and singlet character[2,38]; i.e., cross sections which rise rapidly near threshold and decrease rapidly at energies beyond the maximum and cross sections which rise slowly with energy to a peak near that of the ionization cross section. If the gas density is not too high the triplet states will radiate to the $b^3\Sigma_u^+$ state and the molecule will dissociate, whereas the singlet states will radiate to the ground state. We have chosen to approximate the electronic excitation cross sections by two cross sections, a dissociation cross section Q_d with a threshold and an energy loss of 8.85 eV and a "photon" excitation cross section Q_p with a threshold[39] and energy loss of 12 eV. The dissociation cross section, which agrees in magnitude with that of Ramien[35] near threshold and in shape with that of Massey and Mohr,[38] was left constant throughout this calculation. The photon excitation cross section with a threshold at 12 eV and the vibrational excitation cross sections were adjusted to give agreement between the calculated and experimental ionization coefficients. This assumption is arbitrary and means that unless we were fortunate enough to choose the correct dissociation cross section at energies above 12 eV, only a weighted sum of our electronic excitation cross sections is to be compared with, for example, the results of electron beam experiments. In any case, we do not expect the falling portions of our excitation cross sections to be as accurate as the rising portions, and so have not concerned ourselves with requiring that Q_d and Q_p be consistent with theory[38] at high energies, e.g.,

---

[36] It should be noted that at ϵ_K values near 0.2 eV, our calculated ν_u/N values were always below the experimental ones. This suggests that near the vibrational threshold the rotational cross section is somewhat larger than given by the theory discussed above.

[37] For a recent theoretical calculation of the cross section for dissociation see L. A. Edelstein, Nature 182, 932 (1958).

[38] H. S. Massey and C. B. O. Mohr, Proc. Roy. Soc. (London) A135, 258 (1932). Apparently the cross section given for the excitation of the $b^3\Sigma_u^+$ state is too large by a factor of 30. See R. W. Lunt and C. A. Meek, Proc. Roy. Soc. (London) A157, 146 (1936).

[39] This choice of an effective excitation threshold is based largely on the excitation cross section given by W. Lichten, Phys. Rev. 120, 848 (1960).

above 30 eV. In spite of these uncertainties in the detailed cross sections, we believe that the combined electronic cross section derived in this section facilitates a much more accurate evaluation of electron-transport coefficients than was previously[10-12] possible.

Our procedure in deriving the cross sections for this region was, first of all, to obtain as good a fit as possible between the experimental and calculated values of α_i/N for H_2 by adjusting only the Q_V and Q_P curves so as not to alter the situation in region B. Then following the suggestion of Rose,[40] we varied only the vibrational excitation cross section[41] of D_2, and were successful in obtaining satisfactory agreement between experimental and calculated values of α_i. Had we allowed H_2 and D_2 to have different dissociation and photon-excitation cross sections, we should have been able to derive a bewildering multiplicity of cross sections for D_2, all of which would give comparable agreement between theory and experiment.

Two other assumptions inherent to our analysis can conceivably cause significant errors. The first is that we neglect the presence of the extra electron which is produced in the ionization process. In order to minimize this error, we have limited our calculations to values of E/N for which less than approximately 10% of the total energy input from the field to the electrons was dissipated in the ionization process. An approximate analysis of the magnitude of the terms neglected in the Boltzmann equation analysis indicates that as long as E/N is so restricted the error should not be important. Another cause of possible error has been investigated recently by Baraff and Buchsbaum (BB)[42] who have studied the departure of the electron distribution function from spherical symmetry for high E/N. Our approach and in particular Eq. (2) is based on the Lorentz approximation[5] which assumes that f can be represented adequately be a two-term expansion in spherical

FIG. 8. Ionization coefficient α_i/N for H_2 and D_2 and electronic excitation coefficient α_e/N for H_2 as a function of E/N. The theoretical results are shown as smooth curves and the experimental ones as points.

harmonics; i.e., the distribution function is not far from being spherically symmetric. The essential conclusion of the BB analysis as it affects our approach is that below an E/N of approximately 1.5×10^{-15} V-cm² the Lorentz approximation is valid. Quite fortuitously, this value of E/N was the one we adopted as an upper bound in order to keep the power dissipated in the ionization process from exceeding 10% of the total.

Our calculated values of α_i/N for both H_2 and D_2 are shown in Fig. 8 as smooth curves. The agreement with the experimental data of Rose[40] and Frommhold[29] is excellent. Also shown in Fig. 8 is a comparison of our calculated values of the total electronic-excitation coefficient[43] α_e/N and the experimental values of Poole[44] for the dissociation coefficient α_d/N. In this figure we have plotted the calculated total electronic-excitation coefficient rather than the dissociation coefficient to emphasize the fact that we do not claim to have separated the effects of dissociation and higher state excitation. The comparison we have made is valid in the range of E/N of Fig. 8, since Corrigan and von Engel[11] have shown that the photon-excitation coefficient is only about 30% of the dissociation coefficient. Our calculated "photon" excitation coefficient is about 10% of the calculated values of α_d at $E/N < 7 \times 10^{-16}$ V-cm². The relatively large experimental photon-excitation coefficient, which was overlooked at the time of our calculations, and the unusual shape, i.e., the prolonged very

[40] D. J. Rose, Phys. Rev. 104, 273 (1956). This paper summarizes the experimental data available at that time.

[41] Our assumption of the same dissociation and photon excitation cross sections for H_2 and D_2 neglects a difference discussed by Condon. See E. U. Condon, Am J. Phys. 15, 365 (1947). The potential energy curves are quite accurately the same in the two isotopic molecules of H_2 and D_2. However, because of its larger mass, the Franck-Condon region for the ground state of D_2 is narrower than that of H_2. This results in differences in the overlap integrals between the $X^1\Sigma_g$ ground state and the excited states, and in differences in the energy dependence of the dissociation and photon-excitation cross sections. We assume that when the differences in the cross sections are averaged over the distribution function the effective difference is too small to be significant in our calculations.

[42] G. A. Baraff, Bull. Am. Phys. Soc. 7, 633 (1962); and G. A. Baraff and S. J. Buchsbaum, Phys. Rev. 130, 1007 (1963). Baraff and Buchsbaum used the Q_V, Q_d, and Q_p curves of Figs. 2 and 7 to calculate ionization coefficients for $E/N > 1.1 \times 10^{-15}$ V-cm². However, their use of a Q_m different from that of Fig. 2 leads to a discrepancy at the same E/N between their values of the ionization coefficient and our results which agree well with the experimental ones of Rose. This state of affairs exists despite the fact that both theoretical calculations are based on the "minimum energy loss" assumption. The lower ionization coefficients which they obtain with the "maximum energy loss" assumption are expected since our inelastic cross sections would have been lowered had they been calculated for this assumption.
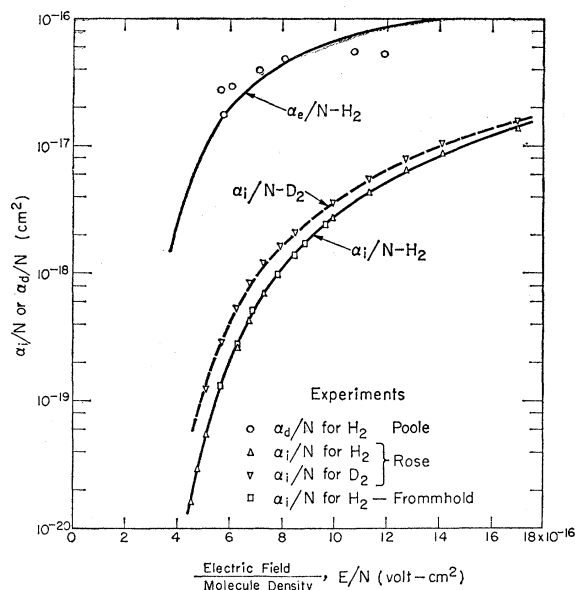
[43] Here α_e is actually $\alpha_d + \alpha_p$ as defined by Eqs. (10) and (10a).

[44] H. G. Poole, Proc. Roy. Soc. (London) A163, 404, 415, and 424 (1937). These results have been comfirmed by Corrigan and von Engel (Ref. 11) and by T. M. Shaw, J. Chem. Phys. 30, 1366 (1959).
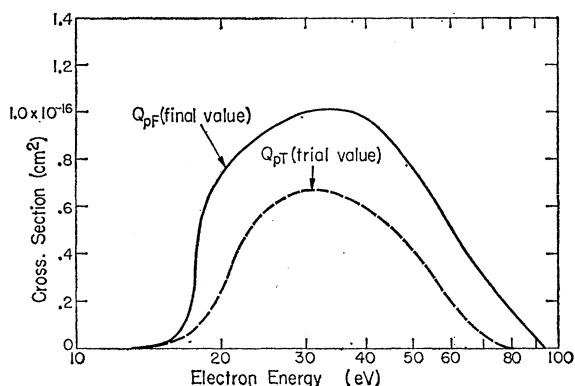
FIG. 9. A trial value Q_{pT} and the final value Q_{pF} of the photon-excitation cross section for H_2 plotted against electron energy.

small cross section near threshold of the Q_p curve of Fig. 9, are the basis of our emphasis on the "total" excitation cross section and rates rather than the separate dissociation and photon contributions.

The sensitivity of this method of determining cross sections is illustrated by Fig. 10 where the results of four cases using different combinations of Q_V and Q_p for H_2 are plotted. The ionization coefficient ratio R_i is the ratio of the calculated value of α_i/N to the experimental one of Rose at the same value of E/N. The trial value Q_{VT} of the vibrational excitation cross section differs from the final value Q_{VF} only above 3 eV (see Fig. 1); the former exceeds the latter by about 7% at the peak which occurs at 4.5 eV. As shown in Fig. 9, the trial value Q_{pT} of the electronic excitation cross section is less than the final value Q_{pF} at all energies; the latter exceeds the former by about 35% at the peak which occurs at 33.0 eV. Q_{po} is a photon-excitation cross section which is identically zero for all electron energies.

The results of case (i) are much too high. However, by increasing the photon-excitation cross section from zero to Q_{pT}, we improve this situation considerably although the discrepancy in R_i at high E/N is still quite large. Case (iii) illustrates that decreasing the cross section for vibrational excitation from Q_{VT} to Q_{VF} improves the shape of the calculated curve by making the fractional error nearly constant. Moreover, the shift in the calculated points caused by changing Q_V but not Q_p indicates that α_i/N is rather sensitive to Q_V at lower values of E/N but not at higher ones. The final adjustment made by using Q_{pF} instead of Q_{pT} results in excellent agreement with a maximum discrepancy of about 5%. A similar procedure was followed for D_2 with the exception that Q_p was held constant at the value Q_{pF} and Q_V was varied in such a way as to minimize the discrepancy and not to perturb the fit in region B. In the case of D_2 we were able to fit the experimental α_i/N values to about 15%. {*Note added in proof*. Cottingham and Buchsbaum have recently reported [Sixth International Conference on Ionization Phenomena in Gases, Paris, 1963 (to be published)] that the ν_i values for electrons in H_2 and

D_2 are very nearly the same. This result appears to be in contradiction to that of Ref. 40. If the ionization frequencies for H_2 and D_2 are the same, then our procedure would lead to identical vibrational and electronic excitation cross sections for H_2 and D_2 at energies above about 3 eV.}

The relative importance of the various energy-loss processes in region C is elaborated somewhat further in Fig. 11, where we plot the ratio of the power input dissipated by a process to the total power given by the field to the electrons. Thus P_l, P_V, and P_i are, respectively, the fractional power input values for elastic scattering, vibrational excitation, and ionization; P_e is the sum of the fractional power input values to dissociation and photon excitation. First of all, we note that P_l and P_V for H_2 are greater than the corresponding quantities for D_2, whereas the converse is true for P_e and P_i. We would expect P_l to be smaller for D_2 because the molecular mass of D_2 is twice as great as that of H_2; i.e., the $2m/M$ factor before the second term of Eq. (2) is reduced. Similarly P_V for D_2 is smaller partly because of the smaller threshold energy of 0.36 eV, and partly because of the smaller D_2 cross section for vibrational excitation. Finally, we note that P_V is much greater than P_e at the lowest values of E/N, whereas at the highest values P_e exceeds P_V but not by a considerable factor. Consequently, vibrational excitation is important over this entire range of E/N in determining α_i/N. This is contrary to the conclusion reached by Allis and Brown[45] but consistent with that of Rose[40] and Heylen and Lewis.[12]

In contrast to the very satisfactory agreement obtained for α_i/N, the plots of ν_m/N and ν_u/N for H_2 exhibit some very definite discrepancies. In the case of the ν_u/N curve, our computed points are well below the experimental curve. Calculations have been performed wherein it was attempted to obtain a better fit to the
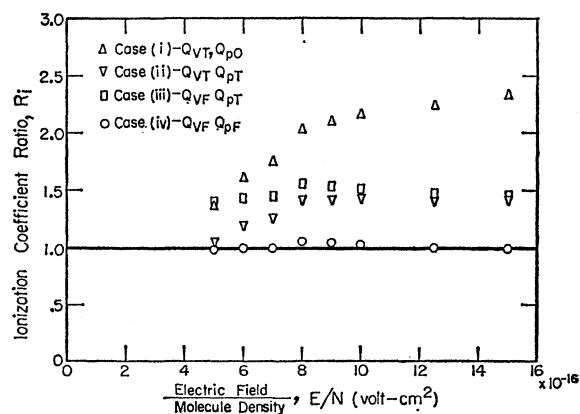

FIG. 10. The ionization coefficient ratio R_i for H_2 as a function of E/N for various combinations of vibrational and photon-excitation cross sections. Q_{VT} and Q_{VI} are shown in Fig. 1, whereas Q_{pT} and Q_{pF} are plotted in Fig. 9. Q_{po} is a photon excitation cross section which is zero at all energies.

[45] W. P. Allis and S. C. Brown, Phys. Rev. 87, 419 (1952).

ν_u/N curve by increasing Q_V. However, it became apparent that an increased Q_V would preclude entirely the possibility of agreement in the case of α_i/N, and as a result, such an approach was abandoned. This discrepancy in ν_u/N is also evident in the ϵ_K plot of Fig. 5 for H_2 where for $\epsilon_K>1.5$ eV our calculated curve lies significantly above the experimental points. In the case of ν_m/N, the discrepancy is small up to $\epsilon_K=2.0$ eV, but for greater values of ϵ_K the experimental curve actually starts to drop, whereas the calculated points are almost constant. This result appears to argue for a smaller Q_m at high energies which in turn would tend to increase our inelastic cross sections obtained by requiring agreement between experimental and theoretical values of α_i/N. In the absence of adequate ϵ_K data we have been reluctant to decrease Q_m. Our calculations in region C of w, ϵ_K, ν_m/N, and ν_u/N for D_2 are shown in Figs. 4 and 6, although no experimental results are available at this time.

Now that we have obtained a fit between the experimental and computed ionization coefficients, it is pertinent to ask in what way our result in region C represents an improvement over previous results. First, we will compare our results with those of Lunt and Meek.[10] These authors were able to obtain a satisfactory, although not extremely good, fit to the available ionization coefficient data using a Maxwellian distribution of electron energies and the measured values of ϵ_K. Our claim is that the erroneously small
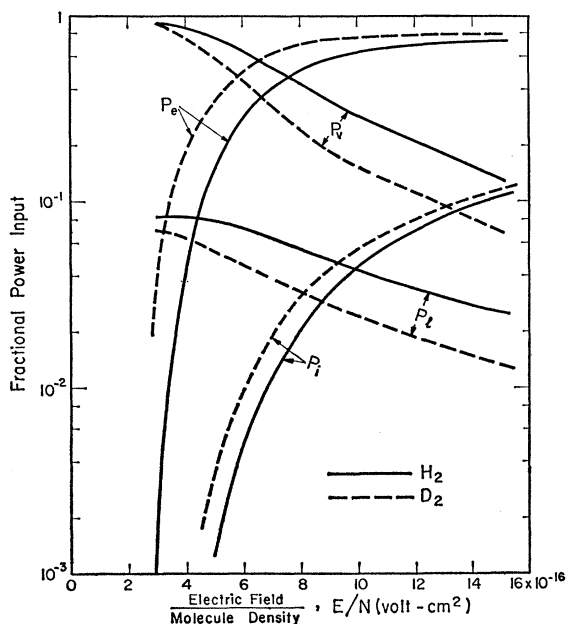

FIG. 12. Comparison of distribution functions of electrons in H_2 for $E/N=9.0\times10^{-16}$ V-cm². The solid curve represents the results of our calculations from which we obtain $\epsilon_K=3.24$ eV. The dashed curve is the Maxwellian distribution for $kT/e=\epsilon_K=2.40$ eV, the value reported by Townsend and Bailey (Ref. 30) and used by Lunt and Meek in their calculations (Ref. 10).

experimental values of ϵ_K due to Townsend and Bailey[30] were sufficient to compensate for the relatively large number of high-energy electrons in a Maxwellian energy distribution, so as to give approximately the correct ionization coefficient. This effect is illustrated in Fig. 12 where we have shown our calculated f and the Maxwellian f for an $E/N=9\times10^{-16}$ V-cm². The α_i/N values are 1.9×10^{-18} and 2.2×10^{-18} cm² for the exact and Maxwellian distributions, respectively. This is rather close when one considers the rather different values of ϵ_K.

Our results in region C differ considerably from those of Heylen and Lewis[12] because we have not forced the computed values of ϵ_K to agree with the experimental data. The net effect of this is that our momentum transfer and electronic excitation cross sections are considerably larger than their values and in agreement with the more direct measurements of the cross section. It should be pointed out that the microwave data of Varnerin and Brown[46] lend support to our belief that the ϵ_K values of Townsend and Bailey are too small.

IV. TRANSPORT COEFFICIENTS FOR AC ELECTRIC FIELDS AND CROSSED ELECTRIC AND MAGNETIC FIELDS

In order to obtain an additional check on the cross sections derived from data obtained with a uniform dc

FIG. 11. Fractional power input to elastic and inelastic collisions for H_2 and D_2 as a function of E/N for $\epsilon_K>1.0$ eV. P_l, P_V, P_e, and P_i are the fractional power inputs to elastic scattering, vibrational excitation, electronic excitation, and ionization, respectively. The P_l term representing elastic collisions is the difference between the energy loss and energy gain terms, i.e., the first integral on the right-hand side of Eq. (9).
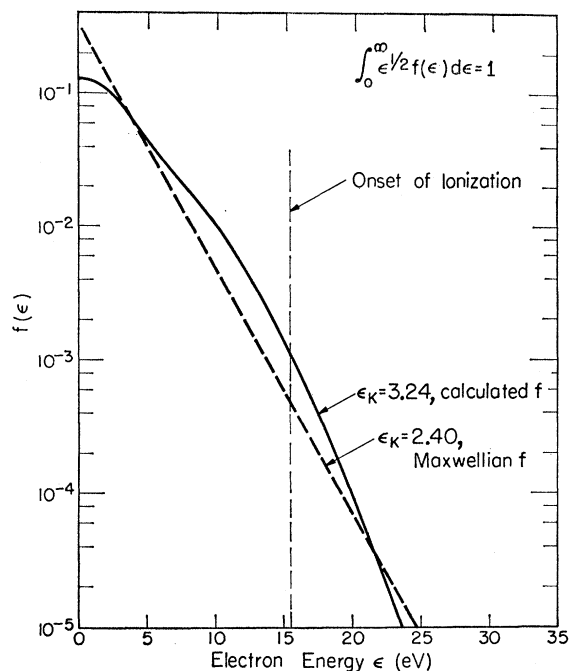
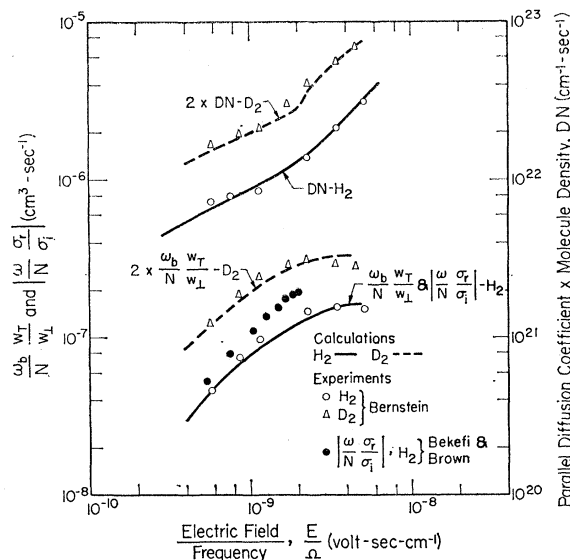[46] L. J. Varnerin and S. C. Brown, Phys. Rev. 79, 946 (1950).

FIG. 13. Parallel diffusion coefficient DN, magnetic drift velocity ratio $(\omega_b/N)(w_T/w_\perp)$, and conductivity ratio $(\omega_b/N)(\sigma_r/\sigma_i)$ for H_2 and D_2. Our calculations are shown as a solid curve for H_2 and a dashed curve for D_2. Bernstein's experimental results for H_2 and D_2 are shown as open points and those of Bekefi and Brown for H_2 only as solid points.

electric field and no magnetic field present, transport coefficients have been calculated for two additional configurations:

(A) crossed electric and magnetic fields, i.e., $\Omega = \omega_b$ in Eq. (4),

(B) ac electric fields, i.e., $\Omega = \omega$.

In the first case a comparison can be made with the experimental results of Bernstein[13] and the theoretical ones for high magnetic fields of Pearson and Kunkel.[14] In the second case the microwave conductivity measurements by Bekefi and Brown,[47] and the recent microwave breakdown measurements of Cottingham and Buchsbaum (CB)[13] are available.

The comparison is facilitated by the definition of an energy-independent effective electric field[5] given by

$$E_e = E(1 + \Omega^2/\nu_c^2)^{-1/2}, \qquad (25)$$

where ν_c is some effective collision frequency. We use E_e here merely for the sake of convenience in plotting results since we do not assume the frequency of momentum transfer collisions, $\nu Q_m N$, to be independent of electron energy. The actual calculation of transport coefficients is accomplished using the more rigorous Eq. (4). However, for H_2 and D_2 in the region above 2 eV it is a reasonably good approximation to say that $Q_m \propto \epsilon^{-1/2}$ or $\nu_c \propto \epsilon^{1/2} Q_m(\epsilon) = \text{const}$. From Fig. 3 it is seen that above 3 eV our calculated value of ν_m/N is almost

[47] G. Bekefi and S. C. Brown, Phys. Rev. 112, 159 (1958). We note that in spite of the disagreement indicated in Fig. 13, the Q_m values obtained by these authors are in good agreement with the values used in our analysis (See Ref. 4).

constant at 1.68×10^{-7} cm³ sec⁻¹. This is the value of ν_c/N we have adopted for insertion into Eq. (25), since it is consistent with the cross sections we have derived and is in good agreement with the value used in previous analyses.[46] Cottingham and Buchsbaum[13] believe a value of $\nu_c/N = 1.36 \times 10^{-7}$ cm³ sec⁻¹ is a better one, because when used in Eq. (25) it leads to slightly better agreement between their ac data and the dc results of Rose.[40]

The comparison of calculated and experimental values of the mobility and diffusion coefficients for H_2 and D_2 at high magnetic fields is shown in Fig. 13 as a plot of $(\omega_b/N)(w_T/w_\perp)$ and DN versus E/Ω, where $\Omega = \omega_b$ or ω. The plots are independent of ω_b/N since the experimental conditions were such that $(w_T/w_\perp)^2 \ll 1$. The agreement between the experimental and calculated values of $(\omega_b/N)(w_T/w_\perp)$ and DN is reasonably good for both H_2 and D_2. Now the ratio of the real to imaginary part of the high-frequency conductivity,[17] viz. σ_r/σ_i, is given by the same integrals as used to evaluate $w_T/w_\perp$ if ω_b is replaced by ω. We, therefore, expect values of $(\omega/N)(\sigma_r/\sigma_i)$ versus E/ω for $(\sigma_r/\sigma_i)^2 \ll 1$ to coincide with the values of $(\omega_b/N)(w_T/w_\perp)$ versus E/ω_b in Fig. 13. However, we see that the experimental microwave data[47] are from 30 to 50% higher than the high-magnetic field data or the calculated values. The source of this discrepancy is unknown.
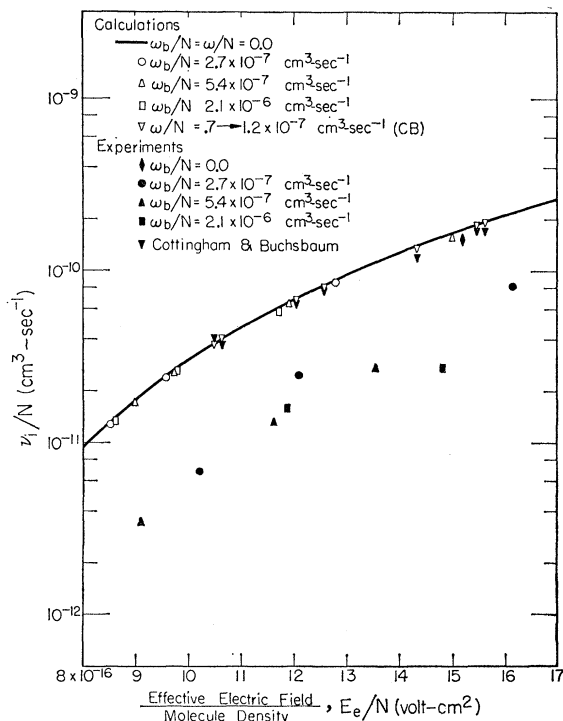

FIG. 14. Ionization frequency ν_i/N for H_2 as a function of the energy-independent effective field E_e/N. The solid curve represents our dc results which agree very well with those of Rose. The open inverted triangles represent the results of our calculations at the same E/N and ω/N as the solid inverted triangles which show the experimental results of Cottingham and Buchsbaum. The remaining points refer to calculations and experiments in crossed electric and magnetic fields.
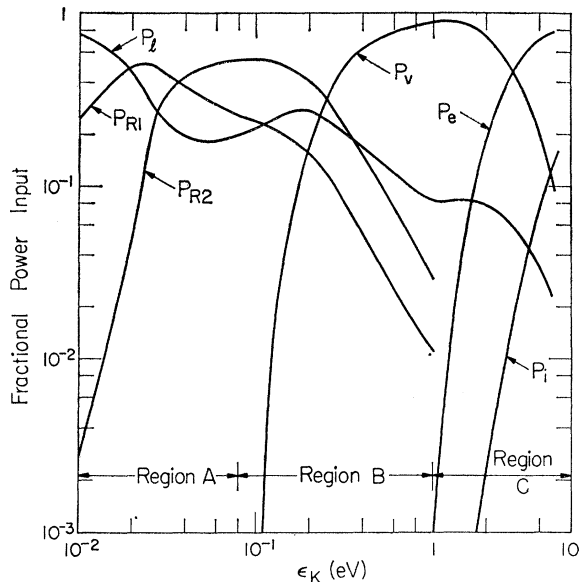
FIG. 15. Fractional power input to elastic and inelastic collisions for H_2 as a function of the characteristic energy ϵ_K which varies through regions A, B, and C. P_l, P_V, P_e, and P_i have the same meaning as in Fig. 13; P_{R1} and P_{R2} are the power inputs at 77°K to the first two rotational levels neglecting inelastic collisions of the second kind.

The most convenient way to compare ionization coefficients for various experimental arrangements is to reduce the results to the ionization frequency ν_i. The theoretical ionization frequency is calculated using Eq. (10). The ionization frequency for the crossed electric and magnetic field experiments is obtained by multiplying the α_i values measured by Bernstein[13] by the electron drift velocity in the direction of the electric field, i.e., the transverse drift velocity, w_T. The transverse drift velocity is used in this case rather than the net drift velocity, $(w_T^2+w_\perp^2)^{1/2}$, since the distance used to calculate the experimental α_i's is in the direction of the electric field. In the ac case, we compare directly with the measured ionization growth constant or frequency. The simplicity in the comparison between the theoretical and experimental data for the ac case would no longer exist if we had made our comparison of ionization coefficients using the Townsend α coefficients, since it would be necessary then to define an effective drift velocity.

Figure 14 displays plots of ν_i/N for H_2 for both configurations A and B. The solid line represents our results for only a dc electric field present, and, as shown in Fig. 8, agrees quite well with the results of Rose.[4] In the case of an ac electric field present, shown are the results of Cottingham and Buchsbaum,[13] and our calculations which were done for the same pressure, microwave frequency, and electric field as the CB experiment. There is virtually no discrepancy between our calculated points for this case and the solid line. Within the scatter of the experimental data the CB results show little departure from the solid curve, although their data can be brought into slightly better agreement with that of Rose if $\nu_c/N = 1.36 \times 10^{-7}$ cm³ sec⁻¹ is used instead. However, had we used the lower value of ν_c/N in Eq. (25), then our ac results would fall approximately 20% above the dc curve, and our ω_b/N data would be even higher. This illustrates the necessity for consistency between the Q_m data used in both the theoretical and experimental analyses.[42]

Greater and more significant discrepancies are present for the situation of crossed electric and magnetic fields. On the one hand, our calculated results for three non-zero values of ω_b/N shown are within 5% of the curve for $\omega_b/N = 0$. On the other hand, although Bernstein's experimental values for $\omega_b/N = 0$ also agree with those of Rose, his results for nonzero magnetic field fall distressingly far from the curve, and therefore his findings are open to question. Further evidence for questioning Bernstein's results is provided by recent calculations by Pearson and Kunkel[14] of α_i for electrons in H_2 subjected to high magnetic fields, e.g., $\omega_b/N = 2.1 \times 10^{-6}$ cm³ sec⁻¹. The method of Pearson and Kunkel is somewhat different from ours since they perform their analysis for a drift frame of reference moving with a velocity $E \times B$. By using cross sections similar to ours Pearson and Kunkel obtain results which are almost identical to ours.

The results shown in Fig. 14 indicate that there is a slight shift of the calculated ν_i/N results towards lower values with increasing Ω/N. For the conditions of CB for which $\omega \leq 0.72\nu_c$, our computed points fall right on the curve. However, with increasing Ω the results are depressed as is shown by the three cases of ω_b/N plotted. Although this trend did not create discrepancies greater than 5%, it does question mildly the concept of the energy-independent effective field. In a sense a degeneracy exists since one value of E_e/N gives rise to more than one value of ν_i/N.

V. DISCUSSION AND SUMMARY

By means of the analysis discussed in previous sections we have derived a set of momentum transfer and inelastic scattering cross sections for electrons in H_2 and D_2. These cross sections are consistent with most of the available experimental data on electron transport coefficients. The assumption of the same Q_m for H_2 and D_2 has been shown to be valid. As an aid to obtaining an over-all view of our calculations we present in Fig. 15 plots of the fractional power input for various energy loss processes in H_2. Since the calculations shown are for $T = 77°K$ in regions A and B, it is necessary to exhibit only the curves for electron energy loss in excitation of the first two rotational states, viz., P_{R1} and P_{R2}. The cross sections for electron energy gain by de-excitation of the rotationally excited molecules are so small that inelastic collisions of the second kind do not make a significant contribution to the energy balance as given

in Eq. (9). In addition, it is worth noting that for a given gas temperature thermal effects do not play an important role for $\epsilon_K > 10kT$. Hence, in region C we have set $T = 300°K$, a temperature which is close to but not exactly that used in experiments.

Whereas for H_2 equally good agreement is obtained both with and without the polarization correction of Dalgarno and Moffet, for D_2 the use of f_R definitely improves the shape of the ν_u/N curves such that tolerably good agreement is obtained. Nevertheless, residual discrepancies in the ν_u/N curve imply that an error as large as 20% may exist in the shape of the theoretical rotational cross sections. In addition, in both H_2 and D_2 we are left with a discrepancy of about 25% between the effective quadrupole moment required to fit transport coefficient data and the values available from other experiments.[24,26]

The magnitude of the fractional power input to elastic collisions compared with that to inelastic collisions is delineated for H_2 in Fig. 15. We see that only at very low electron energies can rotational excitation be neglected; even at $\epsilon_K = 0.01$ eV, P_{R1} is a third as large as P_l. The P_l curve also displays two very interesting humps. The first hump peaks in the vicinity of $\epsilon_K = 0.2$ eV, since this is a region where P_{R1} and P_{R2} are decreasing rapidly and P_V is not yet sufficiently large. The second hump is much less pronounced and occurs at approximately 1.5 eV where P_V is decreasing and P_e and P_i are increasing quickly.

The vibrational cross section derived for H_2 is greater than that for D_2 above 0.7 eV; the reverse is true below 0.7 eV. Although the differences between the Q_V derived for H_2 in this analysis and that previously postulated by Frost and Phelps[4] are not large, it has been possible to detect them, especially in region B where vibrational excitation tends to dominate the picture.

In region C we have obtained the falling part of the cross section for vibrational excitation and the cross section for electronic excitation by comparing calculated and experimental values of the ionization coefficient, and assuming the same Q_d and Q_p for H_2 and D_2. Despite the fact that there is evidence for believing that the Q_m used may be too large at high energies, we have been reluctant to seek a better fit for lack of sufficiently accurate ϵ_K data. Since at 1.0 eV P_{R1} and P_{R2} are only 0.011 and 0.029 and are decreasing precipitously, we consider the neglect of rotational excitation a justifiable assumption.

Finally, we remark that our cross sections are consistent for the most part with recent determinations[13,14,42] of transport coefficients for electrons subjected to high-frequency ac electrical fields, and crossed dc electric and magnetic fields. However, the concept of the energy-independent effective field should be used with some caution since there exists a lack of uniqueness, viz., for differing Ω/N but the same effective field a slight spread is obtained in the calculated values of ν_i/N.